We are IntechOpen, the world's leading publisher of Open Access books Built by scientists, for scientists

4,800
Open access books available

122,000
International authors and editors

135M
Downloads

Our authors are among the

154
Countries delivered to

TOP 1%
most cited scientists

12.2%
Contributors from top 500 universities

CLARIVATE ANALYTICS BOOK CITATION INDEX INDEXED

WEB OF SCIENCE™

Selection of our books indexed in the Book Citation Index in Web of Science™ Core Collection (BKCI)

Interested in publishing with us?
Contact book.department@intechopen.com

Numbers displayed above are based on latest data collected.
For more information visit www.intechopen.com

19

Nonlinear Conversion Enhancement for Efficient Piezoelectric Electrical Generators

Daniel Guyomar and Mickaël Lallart
Université de Lyon, INSA-Lyon, LGEF EA 682, F-69621, Villeurbanne
FRANCE

1. Introduction

Although primary batteries have initially promoted the development of low-power devices, recent progresses in microelectronics and in ultra-low power system have shown the limit of such a powering solution. In particular, the limited lifespan and complex recycling process of batteries may raise environmental issues as well as maintenance problems for widespread devices. Hence, in order to counteract these drawbacks, recent trends encouraged the research on renewable energy. The possibility of using ambient sources has thus become an important research field (Roundy and Wright, 2004; Krikke, 2005; Ng and Liao, 2005; Paradiso and Starner, 2005; Guyomar *et al.*, 2007a; Lallart *et al.*, 2008a). Such alternative solutions for providing electrical energy to systems may include solar energy (Hamakawa, 2003), thermal energy (Sodano *et al.*, 2006) or mechanical energy. When dealing with small-scale systems, the latter energy source has been of particular interest as vibrations are widely available in many environments (Shearwood and Yates, 1997; Beeby *et al.*, 2007). In addition, the use of piezoelectric transducers for converting mechanical energy into electricity has attracted much attention as such materials offer high energy densities and promising integration potentials, making them a premium choice for the conception of embeddable microgenerators (Anton and Sodano, 2007; Blystad, Halvorsen and Husa, 2008).
However, mechanical energy is still limited in structures, and piezoelectric transducers present moderate coupling coefficients, especially when used in flexural solicitation which is the most common application of such materials when used in energy harvesting applications (Keawboonchuay and Engel, 2003; Richards *et al.*, 2004). Therefore, in order to dispose of efficient devices able to provide a significant amount of energy for powering electronic systems, it is mandatory to enhance the conversion abilities of piezoelectric elements.
To do so, many studies have focused on the material itself, aiming at increasing the piezoelectric activity. In this domain, most of the works performed have consisted in the development of single crystals, which exhibits piezoelectric coefficients d_{31} and g_{31} typically 9 and 4 times higher, respectively, than conventional piezoceramics, leading to performance in terms of energy harvesting 20 times greater (Park and Hackenberger, 2002; Badel *et al.*, 2006a). However, the synthesis procedure for obtaining piezoelectric single crystals is quite complex and not industrializable yet, making them difficult to achieve in large quantities as well as costly. Therefore, the realistic implementation of piezoelectric transducers for energy harvesting purposes necessitates a simpler process. To address this issue, Guyomar *et al.* (2005) proposed a nonlinear treatment for artificially enhancing the conversion abilities of

such materials. The principles of this approach, originally applied for vibration damping purposes (Richard et al., 1999; Petit et al., 2004; Qiu, Ji and Zhu, 2009a), is to quickly invert the charges available on the piezomaterial synchronously with the structure motion.
The purpose of this chapter is to expose efficient energy harvesting schemes based on this nonlinear conversion enhancement concept. Several architectures will be presented from the original nonlinear approach, each of them addressing one or several issues for improving the performance of microgenerators (power output, load independency, low voltage systems, broadband excitation performance...), and a comparative analysis between the techniques will also be discussed.
The chapter is organized as follows. Section 2 aims at introducing a simple but realistic model of an electromechanical system that will be used in the following theoretical development, as well as the basic physical principles of the nonlinear approach for improving the conversion abilities of ferroelectric materials. In section 3 the direct application of the nonlinear concept to energy harvesting will be developed. Then section 4 will expose other nonlinear approaches that allow a decoupling of the energy extraction and storage stages, permitting a harvested power independent from the load. Finally, a last architecture based on a bidirectional energy flow and energy injection mechanism will be introduced in section 5, and be demonstrated to offer an "energy resonance" effect thanks to the feedback loop. A particular attention will be placed on the realistic implementation of such microgenerators as well as on systems featuring low voltage output (as piezoelectric elements are particularly interesting for microdevices) in section 6. Because of the similarities between the two conversion effects, the application of the exposed methods to energy harvesting from temperature variation using pyroelectric materials will be discussed in section 7. Finally, section 8 will summarize the obtained results and draw some conclusions about the concepts exposed in this chapter.

2. Modeling & conversion enhancement principles

Before exposing and analyzing the harvesting systems using nonlinear approaches, it is proposed in this section to describe a simple but realistic model developed by Badel *et al.* (2007) of a structure equipped with piezoelectric inserts, along with the physical principles of the nonlinear treatment for enhancing the conversion abilities of piezoelectric materials.
The electromechanical model that will be used in this chapter is based on a simple electromechanically coupled spring-mass-damper system (Figure 1), which however relates quite well the behavior of the system near one of its resonance frequencies. From the Newton's law and piezoelectric constitutive equations, it can be demonstrated under given assumptions[1] that the governing equation of motion and electrical equation are given by (Badel *et al.*, 2007):

$$\begin{cases} M\ddot{u} + C\dot{u} + K_E u = F - \alpha V \\ I = \alpha\dot{u} - C_0\dot{V} \end{cases}, \tag{1}$$

where u, F, V and I respectively refer to the displacement at a given location of the structure, driving force[2], piezoelectric voltage and current flowing out the piezoelectric element. M,

[1]For the model development, the assumptions are based on plane strain behavior (no stress along z-axis), Euler-Bernoulli hypothesis (plane sections remain plane), and similar dynamic and static deformed shapes (Badel *et al.*, 2007).

[2]For seismic systems, the force may also be expressed as a function of the acceleration. In this case, the applied force is given by $\mu_1 Ma$, with a the acceleration, M the dynamic mass and μ_1 a correction factor (Erturk and Inman, 2008).

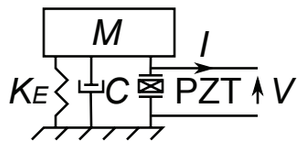

Fig. 1. Single Degree Of Freedom (SDOF) model of an electromechanical structure

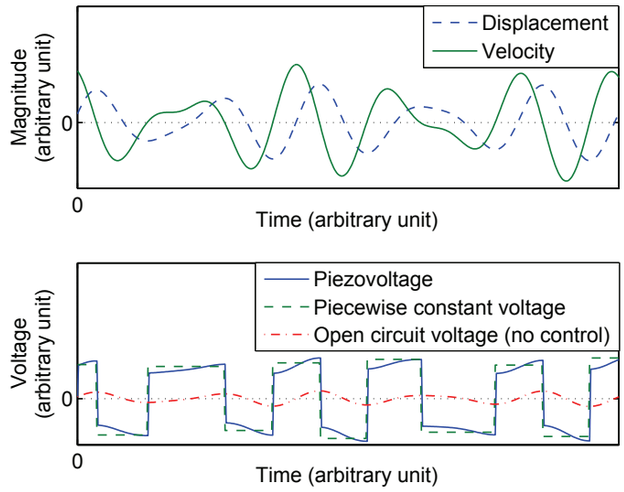

Fig. 2. Waveforms using nonlinear treatment

C and K_E are defined as the dynamic mass, structural damping coefficient and short-circuit stiffness, and α and C_0 are given as the force factor and piezocapacitance. In open circuit condition, it is also possible to define an open-circuit stiffness K_D, whose expression yields:

$$K_D = K_E + \frac{\alpha^2}{C_0}. \tag{2}$$

The energy analysis over a particular time range $[t_0; t_0 + \tau]$ therefore yields:

$$\begin{cases} \int_{t_0}^{t_0+\tau} F\dot{u}dt = \frac{1}{2}M\left[\dot{u}^2\right]_{t_0}^{t_0+\tau} + C\int_{t_0}^{t_0+\tau}\dot{u}^2dt + \frac{1}{2}K_E\left[u^2\right]_{t_0}^{t_0+\tau} + \alpha\int_{t_0}^{t_0+\tau}V\dot{u}dt \\ \alpha\int_{t_0}^{t_0+\tau}V\dot{u}dt = \int_{t_0}^{t_0+\tau}VIdt + \frac{1}{2}C_0\left[V^2\right]_{t_0}^{t_0+\tau} \end{cases}. \tag{3}$$

Hence, it can be seen that from the motion equation that the amount of converted energy is given by the time integral of the product of the voltage by the velocity. Therefore, in order to increase the converted energy, two possibilities may be adopted[3]:

– Increase the voltage magnitude

– Ensure that the voltage is as proportional as possible to the speed (*i.e.*, reduce the time shift between V and $\dot{u}$).

To do so, several approaches are possible, but they have to consume as less energy as possible. In particular, inverting the piezovoltage on its maximum and minimum value allows shaping an additional piecewise constant voltage proportional to the sign of the velocity much larger than the original voltage (Figure 2). Such a process therefore allows benefitting from both effects for improving the conversion.

[3]considering that the velocity remains constant

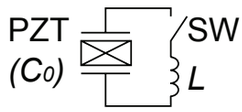

Fig. 3. Implementation of the inversion process

The inversion process can besides be obtained in a very simple way without requiring any external energy. The principles of this process lie on the dielectric properties of piezoelements. Thanks to their capacitive behavior, the voltage is continuous. Hence, after an inversion event, the induced initial condition change is kept on the material, shaping the piecewise function. The inversion process is very simple as well. It consists in connecting the piezoelectric element to an inductor L (Figure 3), which creates an oscillating network. Hence, once the piezoelectric element is connected to the inductance, the voltage starts oscillating around 0, and, if the switching time t_i is chosen so that it equals half the electrical oscillation pseudo-period:

$$t_i = \pi\sqrt{LC_0}, \tag{4}$$

this leads to an inversion of the piezoelectric voltage. This inversion process is however not perfect because of the losses in the circuit, and can be characterized by the inversion coefficient γ giving the ratio of the absolute voltages before and after the inversion, which can also be obtained from the electrical quality factor Q_i of the LC_0 network:

$$\gamma = e^{-\frac{\pi}{2Q_i}} \text{ with } Q_i = \frac{1}{r}\sqrt{\frac{L}{C_0}}, \tag{5}$$

with r the equivalent loss resistance of the circuit.

3. SSH techniques

Now the basic principles of the nonlinear conversion enhancement exposed, this section proposes the direct application of this concept to energy harvesting, leading to the concept of *Synchronized Switch Harvesting on Inductor* (Guyomar *et al.*, 2005; Lefeuvre *et al.*, 2006a; Shu, Lien and Wu, 2007; Liang and Liao, 2009; Qiu *et al.*, 2009b). Considering the standard energy harvesting interface that consists in connecting the piezoelectric element to a smoothing capacitor C_S and load R_L (that represents the connected device) through a diode bridge rectifier (Figure 4(a)), the switching element may be placed in two ways:

– In parallel with the piezoelectric element (Parallel SSHI - Figure 4(b))

– In series with the piezoelectric element and the harvesting stage (Series SSHI - Figure 4(c))

When using the standard interface, it can be demonstrated that the harvested energy under a constant vibration magnitude u_M is given in steady state case by (Guyomar *et al.*, 2005):

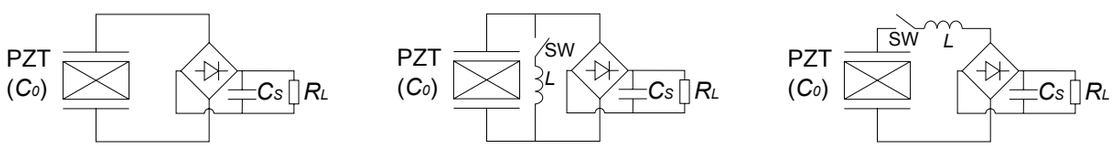

(a) Standard (b) Parallel SSHI (c) Series SSHI

Fig. 4. Energy harvesting interfaces

$$P_{\text{standard}} = \frac{(4\alpha f_0)^2 R_L}{(1+4f_0 C_0 R_L)^2} {u_M}^2, \tag{6}$$

with f_0 and u_M referring to the vibration frequency and displacement magnitude, respectively. The associated maximal power when using the optimal load yields:

$$P_{\text{standard}}|_{\max} = f_0 \frac{\alpha^2}{C_0} {u_M}^2. \tag{7}$$

However, converting mechanical energy into electrical energy decreases the former, therefore leading to vibration damping effect that limits the effective harvested power. When considering that the system is submitted to a monochromatic driving force with constant magnitude F_M, an energy analysis of the system leads to the expression of the power (Guyomar *et al.*, 2005):

$$P_{\text{standard}} = \frac{(4\alpha f_0)^2 R_L}{(1+4f_0 C_0 R_L)^2} \left(\frac{F_M}{2\pi C f_0 + \frac{16\alpha^2 f_0 R_L}{\pi + (1+4f_0 C_0 R_L)^2}} \right)^2, \tag{8}$$

whose maximal value is given by:

$$\begin{cases} P_{\text{standard}}|_{\max} = \frac{k^2 Q_M}{(\pi + k^2 Q_M)^2} \frac{\pi}{2} \frac{{F_M}^2}{C} & \text{for } k^2 Q_M \leq \pi \\ P_{\text{standard}}|_{\max} = \frac{{F_M}^2}{8C} & \text{for } k^2 Q_M \geq \pi \end{cases}, \tag{9}$$

where $k^2 Q_M$ represents the figure of merit given by the product of the mechanical quality factor Q_M:

$$Q_M = \frac{\sqrt{K_D M}}{C}, \tag{10}$$

representing the amount of mechanical energy that can be converted, by the squared coupling coefficient k^2:

$$k^2 = \frac{\alpha^2}{C_0 K_D}, \tag{11}$$

which gives the part of mechanical energy that can effectively be converted into electrical energy.

3.1 Parallel SSHI

The principles of parallel SSHI (Guyomar *et al.*, 2005) consist of inverting the voltage of the piezoelectric element when the velocity cancels. Hence, such an operation leads to three steps in the conversion and harvesting process (Figure 5):

1. Open-circuit phase (step (1) in Figure 5)
2. Harvesting phase (step (2) in Figure 5)
3. Inversion phase (step (3) in Figure 5)

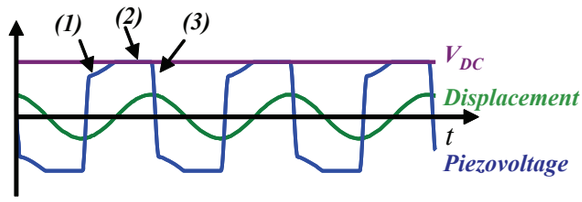

Fig. 5. Parallel SSHI waveforms

The energy harvested using the parallel SSHI approach over a single scavenging cyle may be expressed by:

$$E_{\text{pSSHI}} = \int_{t_1}^{t_1+\tau} V_{DC} I dt, \tag{12}$$

where V_{DC} refers to the rectified voltage (assumed constant as the time constant $R_L C_0$ is far greater than half a vibration period $T/2$) and I the current flowing from the piezoelectric element to the storage stage. t_1 and $t_1 + \tau$ respectively refer to the time when the harvesting process starts (absolute piezovoltage equals to the rectified voltage) and stops (current cancellation, occurring coincidentally with displacement minimum or maximum values). From the electrical equation of Eq. (1), the harvested energy yields:

$$E_{\text{pSSHI}} = \alpha V_{DC} \left(u_M - u_1 \right), \tag{13}$$

with u_1 and u_M the displacement value when the rectifier starts conducting and displacement magnitude, respectively. The value of u_1 may be found by integrating the current equation during the open circuit phase ($I = 0$), and considering that the voltage varies from γV_{DC} (which corresponds to a displacement $-u_M$) to V_{DC} (Figure 5):

$$u_1 = \frac{C_0}{\alpha} \left(1 - \gamma \right) V_{DC} - u_M, \tag{14}$$

leading to the expression of the harvested power as a function of the rectified voltage and displacement magnitude:

$$P_{\text{pSSHI}} = 2 f_0 E_{\text{pSSHI}} = 2 f_0 V_{DC} \left(2 \alpha u_M - C_0 \left(1 - \gamma \right) V_{DC} \right). \tag{15}$$

Noting that the power may also be given by $P = {V_{DC}}^2 / R_L$, the harvested power may also be expressed using the load value:

$$P_{\text{pSSHI}} = \frac{\left(4 f_0 \alpha \right)^2 R_L}{\left(1 + 2 \left(1 - \gamma \right) R_L C_0 f_0 \right)^2} {u_M}^2. \tag{16}$$

Nevertheless, converting mechanical energy into electricity leads to a reduction of the vibrations. Because of this damping effect, less energy is available from the source when the system is driven by a constant force magnitude. In this case, the energy analysis of the equation of motion allows expressing the displacement magnitude in steady state case, assuming an excitation at the resonance frequency:

$$\int_{t_0}^{t_0+T/2} F \dot{u} dt = C \int_{t_0}^{t_0+T/2} \dot{u}^2 dt + \frac{1}{2} C_0 \left(1 - \gamma^2 \right) {V_{DC}}^2 + \frac{T}{2} \frac{{V_{DC}}^2}{R_L}, \tag{17}$$

where the left side member is the provided energy, and the right side members the dissipated energy (through mechanical losses), energy lost in the switching circuit, and harvested energy.

Assuming that the system features relatively high mechanical quality factor ($Q_M > 10$), the velocity and force may be considered in phase at the resonance, yielding the displacement magnitude:

$$u_M\big|_{\text{pSSHI}} = \frac{F_M}{2\pi C f_0 + \frac{16\alpha^2 R_L f_0 (R_L C_0 f_0 (1-\gamma^2)+1)}{\pi (1+2R_L C_0 f_0 (1-\gamma))^2}}, \tag{18}$$

The maximal power harvested taking into account the damping effect may also be approximated as a function of the figure of merit $k^2 Q_M$ as (Guyomar *et al.*, 2009):

$$P_{\text{pSSHI}}\Big|_{\max} \approx \frac{k^2 Q_M}{\pi (1-\gamma) + 8k^2 Q_M} \frac{{F_M}^2}{C}. \tag{19}$$

3.2 Series SSHI

The principles of operation of the series SSHI (Taylor *et al.*, 2001; Lefeuvre *et al.*, 2006a) are a little bit different than in the case of the parallel SSHI. Actually in the case of the series SSHI, the harvesting process occurs at the same time than the inversion process (Figure 6), this latter being done with respect to $+V_{DC}$ (switching from positive voltage) or $-V_{DC}$ (switching from negative voltage).
Therefore the energy harvested over a single switching process yields:

$$E_{\text{sSSHI}} = C_0 V_{DC} (V_M + V_m), \tag{20}$$

with V_M and V_m the absolute values of the voltage just before and after the switching process (Figure 6), whose values may be found considering the inversion process (with respect to V_{DC}):

$$V_m + V_{DC} = \gamma (V_M - V_{DC}), \tag{21}$$

as well as the open-circuit stage between two switching events:

$$V_M - V_m = 2\frac{\alpha}{C_0} u_M. \tag{22}$$

Hence, from Eqs. (20), (21) and (22), the harvested power using the series SSHI approach yields:

$$P_{\text{sSSHI}} = 4\frac{1+\gamma}{1-\gamma} (\alpha u_M - C_0 V_{DC}), \tag{23}$$

which can also be expressed as a function of the load:

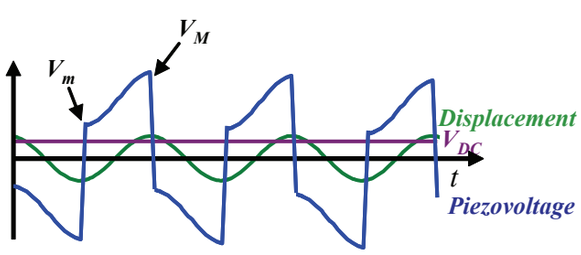

Fig. 6. Series SSHI waveforms

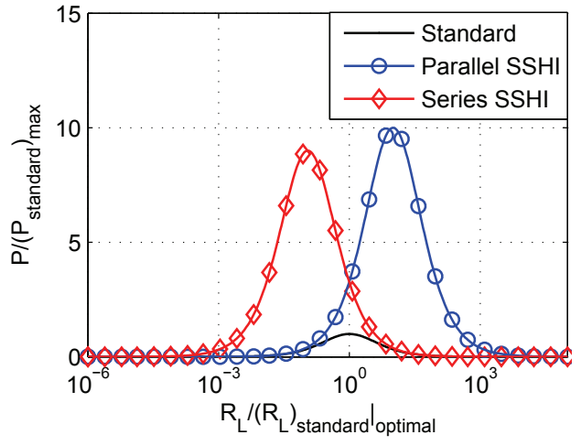

Fig. 7. Normalized harvested power of SSH techniques under constant displacement magnitude and comparison with standard interface ($\gamma = 0.8$)

$$P_{\text{sSSHI}} = \frac{\left(4\left(1+\gamma\right)\alpha f_0\right)^2 R_L}{\left(\left(1-\gamma\right)+4\left(1+\gamma\right)R_L C_0 f_0\right)^2} {u_M}^2. \tag{24}$$

In the same fashion that the standard and parallel SSHI cases, harvesting energy induces vibration damping effect, meaning that less mechanical energy is available for harvesting. From an energy analysis of the system, assuming the structure excited at its resonance frequency by a force with a constant magnitude F_M :

$$\int_{t_0}^{t_0+T/2} F\dot{u}dt = C\int_{t_0}^{t_0+T/2} \dot{u}^2 dt + \frac{1}{2}C_0\left(1-\gamma^2\right)\left(V_M - V_{DC}\right)^2 + \frac{T}{2}\frac{{V_{DC}}^2}{R_L}, \tag{25}$$

it is possible to derive the displacement magnitude taking into account this damping effect:

$$u_M|_{\text{sSSHI}} = \frac{F_M}{2\pi C f_0 + \frac{4\alpha^2(1+\gamma)}{\pi C_0\left((1-\gamma)+4(1+\gamma)R_L C_0 f_0\right)}}. \tag{26}$$

It can also be noted that the effect of the series SSHI can also be seen as the semi-active SSDV[4] damping approach (Badel *et al.*, 2006b; Lefeuvre *et al.*, 2006b), but with a negative voltage. It can besides be shown that the maximal harvested power at the resonance when considering the damping effect may be approximated by (Guyomar *et al.*, 2009):

$$P_{\text{sSSHI}}|_{\max} \approx \frac{k^2 Q_M}{2\pi\frac{1-\gamma}{1+\gamma} + 8k^2 Q_M}\frac{{F_M}^2}{C}. \tag{27}$$

3.3 Discussion

The performance of the SSHI techniques, along with the comparison with the standard interface, are depicted in Figure 7, considering that the electromechanical structure features harmonic displacement with a constant amplitude (*i.e.*, no damping effect). In order to make this chart as independent as possible from the device's parameters, it has been normalized along the x-axis according to the optimal load value in the standard case:

[4] *Synchronized Switch Damping on Voltage source*

$$(R_L)_{\text{standard}}|_{\text{optimal}} = \frac{1}{4f_0C_0}, \tag{28}$$

and along the y-axis according to the maximal power harvested using the standard interface Eq. (7). Therefore, this figure only depends on the inversion coefficient γ that has been set to 0.8; its typical value being comprised between 0.6 and 0.9.

Figure 7 clearly demonstrates the abilities of the SSHI approaches for greatly increasing the power output abilities of the microgenerator, by a typical factor of 9 for the parallel SSHI and a bit less for the series SSHI (8), thanks to the conversion enhancement offered by the switching process[5]. Actually, it can be demonstrated that the converted energy is actually up to 20 times higher than the converted energy in the standard case at the SSHI optimal loads, but the losses in the inversion circuit leads to an efficiency of 50% between the extraction and harvesting stages (Guyomar *et al.*, 2009).

It can also be noted that the optimal load in the parallel SSHI is higher than the optimal load in the standard case, has the nonlinear treatment leads to an artificial decrease of the piezoelectric capacitance value, while the series SSHI features an optimal load less than in the case of the standard technique, which may be beneficial as the capacitive behavior of piezoelectric elements leads to high optimal loads that may be difficult to interface with electronic components.

However, it has previously been pointed out that harvesting energy from a structure driven by a force of constant amplitude at the resonance frequency leads to a vibration damping effect that actually limits the input energy and thus the harvested energy. Figure 8 depicts the normalized harvested power considering such a damping effect, and shows the performance of the nonlinear approaches for harvesting the same amount of energy than in the standard case with much less piezoelectric materials (represented by a lower value of k^2Q_M). However, for highly coupled, weakly damped structures, there is no significant improvement of the nonlinear approaches when considering steady-state excitation and a power limit is reached:

$$P_{\text{lim}} = \frac{{F_M}^2}{8C}, \tag{29}$$

although the SSHI interfaces may be advantageous considering time-limited excitations (Badel *et al.*, 2005a; Lallart, Inman and Guyomar, 2010a). It can also finally be noted that realistic electromechanical structures usually have a value of the figure of merit k^2Q_M less than 1, and therefore can significantly benefit from the nonlinear approach.

It can also be noted from Figure 8 that the optimal loads for both the standard and SSHI approaches change as k^2Q_M increases. Two optimal loads appear for the standard interface after a critical value of k^2Q_M (π), while the optimal load of the parallel SSHI decreases and increases for the series SSHI to reduce the voltage and limit the damping effect, although it also decreases the energy conversion abilities.

Nevertheless, realistic excitations in most of the cases would be barely a sine, but more likely random (Halvorsen, 2008; Blystad, Halvorsen and Husa, 2010). In this case, it can be demonstrated that a trade-off exists between the number of switching events and the value of the voltage at the switching instants, as the extracted energy is proportional to:

$$E_{\text{extracted}} \propto C_0 \sum_k {V_k}^2 \tag{30}$$

[5]It can be shown that the gains of the nonlinear interfaces are given by $2/(1-\gamma)$ and $(1+\gamma)/(1-\gamma)$ for the parallel and series SSHI techniques, respectively.

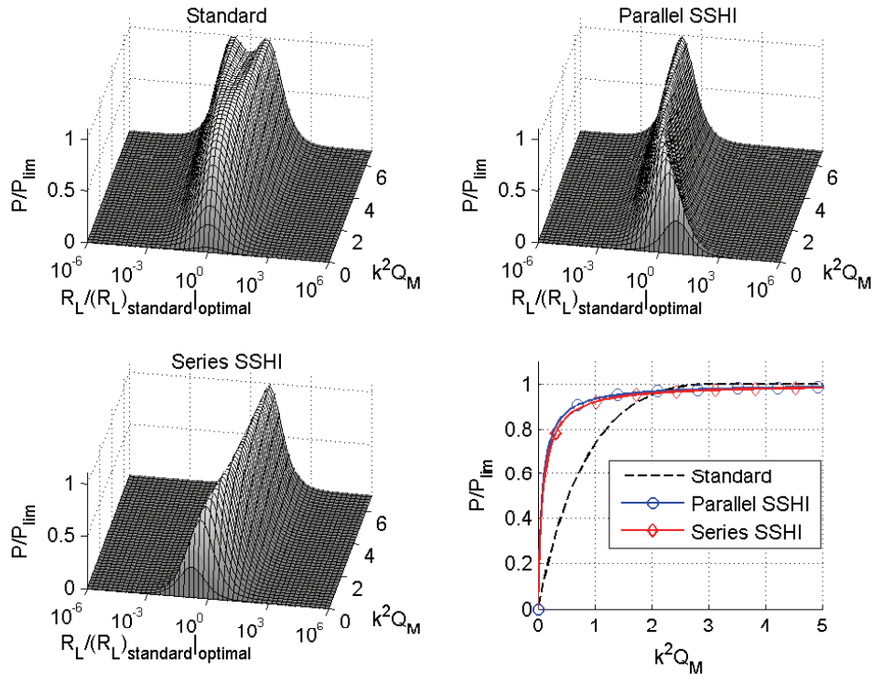

Fig. 8. Normalized harvested power and normalized maximal harvested power of SSH techniques under constant force magnitude and comparison with standard interface ($\gamma = 0.8$)

where V_k denotes the voltage value at the k^{th} instant. This equation shows the trade-off between energy extraction and voltage increase through the cumulative process of the nonlinear technique. Hence, it is possible to improve the SSHI performances in random vibrations by disabling the switch when the voltage or displacement value is less than a user-specified threshold (Guyomar and Badel, 2006; Guyomar, Richard and Mohammadi, 2007b; Lallart *et al.*, 2008b).

4. Charge extraction techniques

The previous section presented the direct application of the nonlinear technique for conversion enhancement to energy harvesting, by connecting the switching element either in parallel (section 3.1) or in series (section 3.2) with the harvesting stage. However, is spite of a great increase of the harvested power, such approaches still suffer from load-dependent power. Hence, the aim of this section is to expose a modified approach still based on nonlinear treatment that not only allows a power output increase (less than the SSHI approaches however), but also a harvested power independent from the load thanks to a decoupling of the extraction stage from the storage, which permits bypassing a supplementary adaptation stage (Ottman *et al.*, 2002; Ottman, Hofmann and Lesieutre, 2003; Han *et al.*, 2004; Lefeuvre *et al.*, 2007a; Lallart and Inman, 2010b) that may dramatically decrease the power because of losses[6].

4.1 SECE technique

The principles of the SECE (*Synchronized Electric Charge Extraction* - Lefeuvre *et al.* (2005)), depicted in Figure 9, consists of extracting all the electrostatic energy available on the

[6]The efficiency of such interface is usually comprised between 70% and 90%.

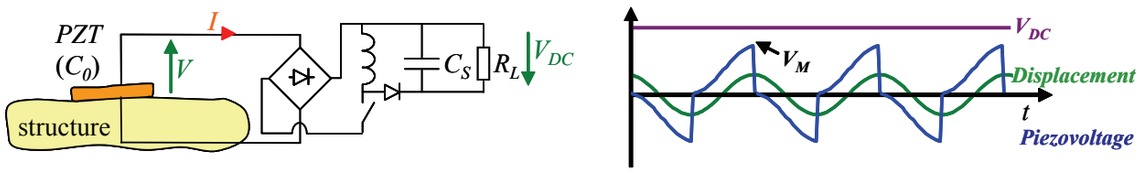

Fig. 9. SECE technique and waveforms

piezoelement when this latter is maximum (otherwise the material is left in open-circuit conditions), which corresponds to minimum and maximum voltages (or equivalently displacement). The extracted energy is then transferred from its electrostatic form into electromagnetic form to an inductance L. After this extraction process, the switch is open and the energy stored in the inductance is transferred to the smoothing capacitor C_S and load R_L. However, because of the losses (mainly in the inductor), a part of the energy is lost.
Hence, for one cycle, the energy extracted is given by:

$$E_{\text{SECE}} = \frac{1}{2} C_0 {V_M}^2, \tag{31}$$

with V_M the piezovoltage just before the harvesting process, whose value can be found considering the open-circuit stage such as:

$$V_M = 2\frac{\alpha}{C_0} u_M. \tag{32}$$

Hence, the harvested power by the SECE technique yields:

$$P_{\text{SECE}} = \gamma_C f_0 \frac{\alpha^2}{C_0} {u_M}^2, \tag{33}$$

with γ_C the efficiency of energy transfer and extraction.
In a purely mechanical point of view, the SECE technique is equivalent to a dry friction, and more particularly to the semi-passive SSDS[7] technique (Badel *et al.*, 2006b). Hence, the damping effect induced by the harvesting process leads to the expression of the displacement magnitude u_M at the resonance frequency:

$$u_M|_{\text{SECE}} = \frac{F_M}{2\pi C f_0 + \frac{4}{\pi}\frac{\alpha^2}{C_0}}, \tag{34}$$

and the associated maximal power at the resonance taking into account the damping effect yields:

$$P_{\text{sSSHI}}|_{\max} = \gamma_C \frac{2}{\pi} \frac{k^2 Q_M}{\left(1 + \frac{4}{\pi} k^2 Q_M\right)^2} \frac{{F_M}^2}{C}. \tag{35}$$

4.2 DSSH technique

The main drawback of the SECE technique lies in the fact that the extraction process cannot be controlled; only all the energy can be extracted. Such a process therefore limits the voltage increase process (as no inversion is performed), hence limiting the conversion enhancement and therefore the harvested energy.

[7] *Synchronized Switch Damping on Short-circuit*

To be able to control the trade-off between extracted energy and voltage increase, as well as the trade-off between energy extraction and damping effect (*i.e.*, the balance between mechanical energy and conversion abilities), it is proposed in this section to use a combination of the series SSHI technique and SECE approach. This concept, called DSSH for *Double Synchronized Switch Harvesting* (Figure 10 - Lallart *et al.* (2008c)), lies in extracting a part of the energy (and use the remaining for processing the voltage inversion) on an intermediate capacitance C_{int}, and then transferring all the energy on C_{int} to the inductance, and finally to the storage stage. When using the DSSH technique, it can be demonstrated that the value of transferred energy to the intermediate capacitor yields (Lallart *et al.*, 2008c):

$$E_{\text{DSSH}}|_{int} = 2x\left(\frac{1+\gamma}{2+(1-\gamma)x}\right)^2 \frac{\alpha^2}{C_0}{u_M}^2, \tag{36}$$

with x the ratio of the intermediate capacitance over the piezocapacitance ($x = C_{int}/C_0$), leading to the expression of the harvested power:

$$P_{\text{DSSH}} = 4f_0 x\gamma_C\left(\frac{1+\gamma}{2+(1-\gamma)x}\right)^2 \frac{\alpha^2}{C_0}{u_M}^2. \tag{37}$$

From Eq. (37), it can be shown that an optimal value of x that maximizes the harvested power under constant vibration magnitude u_M exists ($x_{opt} = 2/(1-\gamma)$), leading to the expression of the maximal power when no damping effect is considered:

$$P_{\text{DSSH}}|_{\text{max}}^{u_M} = f_0\gamma_C\frac{1}{2}\frac{(1+\gamma)^2}{1-\gamma}\frac{\alpha^2}{C_0}{u_M}^2. \tag{38}$$

Another advantage of the DSSH is its ability to control the trade-off between converted energy and damping effect as well. Hence, thanks to its ability to control the amount of extracted energy through the intermediate electrostatic energy tank (intermediate capacitor), the DSSH technique is able to let mechanical energy entering into the system, contrary to fixed system, which, in spite of increasing the conversion abilities of materials, drastically limit the mechanical energy in the system, leading to moderate harvested energy.
In this case, the harvested energy may be expressed as (Lallart *et al.*, 2008c):

$$P_{\text{DSSH}} = \gamma_C\frac{2}{\pi}k^2Q_M\frac{1+\Gamma}{1-\Gamma}\left(\frac{1}{1+\frac{4}{\pi}\frac{1+\Gamma}{1-\Gamma}k^2Q_M}\right)^2\frac{{F_M}^2}{C} \text{ with } \Gamma = -\frac{1-x\gamma}{1+x}. \tag{39}$$

Hence, the trade-off between energy conversion enhancement and input mechanical energy can be tuned through the intermediate capacitor. In particular, an optimal value of x exists that leads to the maximal harvested power at the resonance taking into account the damping effect:

$$\begin{cases} P_{\text{DSSH}}|_{\text{max}} = \gamma_C\frac{2\pi k^2Q_M(1-\gamma^2)}{(\pi(1-\gamma)+4k^2Q_M(1+\gamma))^2}\frac{{F_M}^2}{C} & \text{for } k^2Q_M \le \frac{\pi}{4}\frac{1-\gamma}{1+\gamma} \quad (x_{\text{opt}} = \infty) \\ P_{\text{DSSH}}|_{\text{max}} = \gamma_C\frac{{F_M}^2}{8C} & \text{for } k^2Q_M \le \frac{\pi}{4}\frac{1-\gamma}{1+\gamma} \quad \left(x_{\text{opt}} = \frac{2\pi}{\pi(1-\gamma)+4k^2Q_M(1+\gamma)}\right) \end{cases}. \tag{40}$$

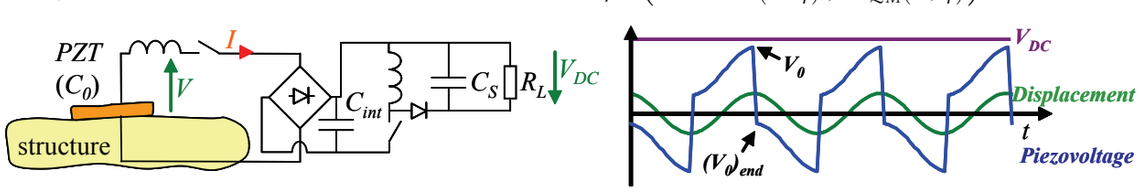

Fig. 10. DSSH technique and waveforms

4.3 Discussion

The performance of the SECE and DSSH techniques considering a monochromatic displacement with a constant amplitude is depicted in Figure 11, which has been normalized in the same way than previously (so that it only depends on the energy transfer efficiency γ_C), with the value of the energy transfer efficiency being given as $\gamma_C = 0.9$. This figure demonstrates that the SECE and DSSH technique allows harvesting 3.5 to 7.5 times more energy than in the standard case, but, in addition to this power output increase, the most remarkable property of these techniques is their independency to the load, which actually leads to performance similar to the SSHI techniques combined with load adaptation interfaces that features typical efficiency of $70 - 90\%$ (Ottman *et al.*, 2002; Ottman, Hofmann and Lesieutre, 2003; Han *et al.*, 2004; Lefeuvre *et al.*, 2007a; Lallart and Inman, 2010b).

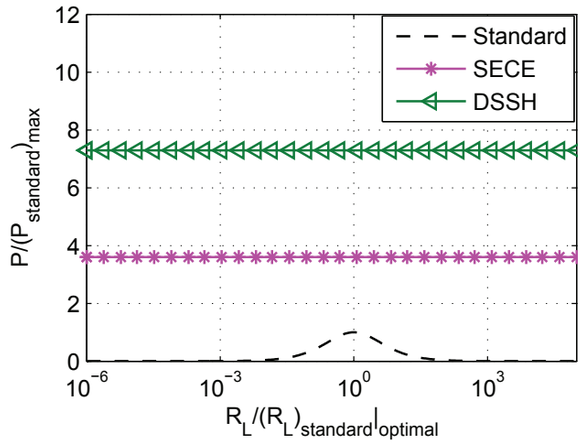

Fig. 11. Normalized harvested power of SECE and DSSH techniques under constant displacement magnitude and comparison with standard interface ($\gamma_C = 0.9$)

When considering the damping effect induced by the energy conversion process, the harvested energy normalized with the power limit (Eq. (29)) is depicted in Figure 12. This chart shows that the SECE is a little bit more efficient than the SSHI techniques for low coupled or highly damped systems (low k^2Q_M), but the power output of this approach is decreasing after reaching an optimal value for large values of k^2Q_M, because the damping effect becomes much larger. This is not the case of the DSSH technique as such a technique allows controlling the trade-off between energy extraction and damping effect through the intermediate capacitance. Such a control also allows the DSSH technique to harvest much more energy for low value of the figure of merit, allowing using up to 10 times less piezoelectric material than the standard interface for realistic values of k^2Q_M. However, although the efficiency of the SECE and DSSH techniques is higher than the SSHI interfaces (Guyomar *et al.*, 2009), the maximal power is less than the power limit because of the energy transfer stage[8].

The SECE and DSSH interface are also very well adapted to multimodal excitation because of the load independency, contrary to the SSHI and standard techniques whose optimal loads depend on the frequency (Lefeuvre *et al.*, 2007b). The SECE technique exhibits relatively

[8]In the case of the standard and SSHI cases, the maximal power would actually be less as well if a load adaptation interface is used to maximize the power.

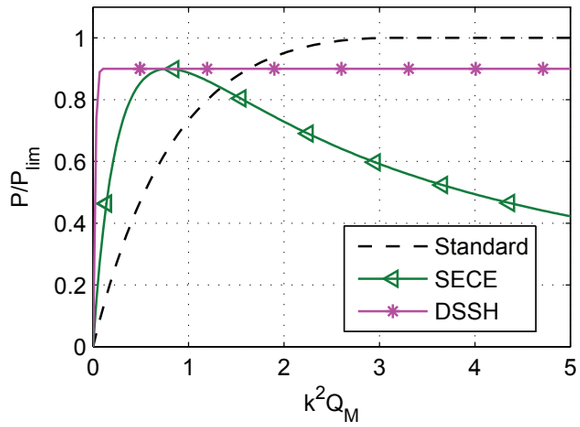

Fig. 12. Normalized harvested power of SECE and DSSH techniques under constant force magnitude and comparison with maximal power of the standard interface ($\gamma_C = 0.9$)

good performances under broadband excitation as well, as this technique relies on voltage cancellation rather than voltage inversion (so that no cumulative process appears).

5. Conversion enhancement and energy harvesting using bidirectional energy transfer and pulsed energy injection

The methods exposed so far considered that once the energy is transferred to the source, it cannot go backward. In this section another concept based on an energy feedback from the storage stage to the source is exposed (Lallart and Guyomar, 2010c). The principles of this method start from the observation that, considering a single energy conversion process, more energy can be converted if an initial energy is given to the system:

$$E_{\text{conv}} = \frac{1}{2} C_0 \left(V_{\text{conv}} + V_{\text{init}}\right)^2 = \frac{1}{2} C_0 {V_{\text{conv}}}^2 + \frac{1}{2} C_0 {V_{\text{init}}}^2 + C_0 V_{\text{conv}} V_{\text{init}}, \tag{41}$$

where V_{conv} is the voltage induced by the conversion process and V_{init} the initial voltage given to the material. In Eq. (41), the first two terms of the right side member respectively correspond to the converted energy without any initial voltage, and initial energy given to the material. Hence, thanks to the quadratic dependence of the energy with the voltage, providing initial energy allows an energy gain given by the cross-product of the two voltage terms, multiplied by the capacitance.
The operations of the energy injection system are as follows (Figure 13):

(1) Energy extraction using SECE technique

(2) Energy injection from the storage stage to the piezoelectric element

(3) Open-circuit

Hence, the energy extracted for a single cycle is given as:

$$E_{\text{extr}} = \frac{1}{2} \gamma_C C_0 {V_M}^2, \tag{42}$$

where V_M is the absolute voltage value when the energy harvesting process is engaged (maximal voltage value) and γ_C the energy transfer efficiency. After this harvesting event, energy is provided from the storage capacitance to the piezoelectric element. In order to

reduce the losses, the energy injection is done through an inductor, leading to the value of the piezoelectric voltage after the process:

$$V_{\text{inj}} = (1+\gamma)\, V_{DC}, \tag{43}$$

with V_{DC} the value of the rectified voltage. Hence, the energy extracted from the source is given by:

$$E_{\text{source}} = (1+\gamma)\, C_0 {V_{DC}}^2. \tag{44}$$

As the piezoelectric element is left in open-circuit condition after the energy injection process, it is therefore possible to derive the value of the voltage V_M as:

$$V_M = (1+\gamma)\, V_{DC} + 2\frac{\alpha}{C_0} u_M, \tag{45}$$

with u_M the displacement magnitude. Hence, the global harvested power using such a technique yields:

$$\begin{aligned} P_{\text{inj}} &= 2 f_0 \left(E_{\text{extr}} - E_{\text{source}}\right) \\ &= f_0 \left[4\gamma_C \tfrac{\alpha^2}{C_0} {u_M}^2 + 4\gamma_C \alpha (1+\gamma)\, u_M V_{DC} + \left(\gamma_C (1+\gamma) - 2\right)(1+\gamma) C_0 {V_{DC}}^2\right]. \end{aligned} \tag{46}$$

which can also be expressed as a function of the load R_L:

$$P_{\text{inj}} = 4 f_0 \gamma_C \left[\frac{(1+\gamma)\sqrt{\gamma_C R_L C_0 f_0} + \sqrt{2(1+\gamma) R_L C_0 f_0 + 1}}{(2-(1+\gamma)\gamma_C)(1+\gamma) R_L C_0 f_0 + 1}\right]^2 \frac{\alpha^2}{C_0} {u_M}^2. \tag{47}$$

Considering that the system is excited at its resonance frequency by a driving force of constant amplitude, the damping effect may be taken into account by considering the mechanical effect similar to the one obtained when using the semi-active SSDV damping approach (Badel *et al.*, 2006b; Lefeuvre *et al.*, 2006b), but with a negative voltage, leading to the expression of the displacement magnitude:

$$u_M|_{\text{inj}} = \left[\frac{1}{1 + \frac{4}{\pi}\left(1 + 2\frac{\gamma_C R_L C_0 f_0 (1+\gamma) + \sqrt{\gamma_C R_L C_0 f_0 (2 R_L C_0 f_0 (1+\gamma)+1)}}{1 + R_L C_0 f_0 (2-(1+\gamma)\gamma_C)(1+\gamma)}\right) k^2 Q_M}\right] \frac{F_M}{2\pi C f_0}, \tag{48}$$

yielding the harvested power:

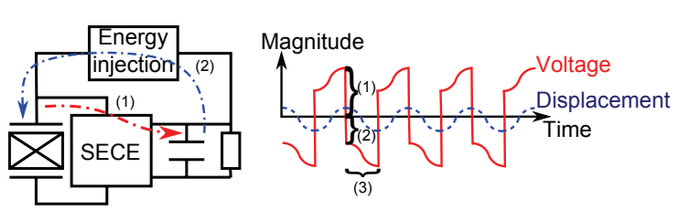

Fig. 13. Bidirectional pulsed energy harvesting principles

$$P_{\text{inj}} = \gamma_C k^2 Q_M \frac{2}{\pi} \frac{{F_M}^2}{C} \left[\frac{(1+\gamma)\sqrt{\gamma_C R_L C_0 f_0} + \sqrt{2(1+\gamma) R_L C_0 f_0 + 1}}{(2-(1+\gamma)\gamma_C)(1+\gamma) R_L C_0 f_0 + 1} \right]^2 \times \left[\frac{1}{1+\frac{4}{\pi}\left(1+2\frac{\gamma_C R_L C_0 f_0 (1+\gamma)+\sqrt{\gamma_C R_L C_0 f_0 \left(2 R_L C_0 f_0 (1+\gamma)+1\right)}}{1+R_L C_0 f_0 \left(2-(1+\gamma)\gamma_C\right)(1+\gamma)}\right) k^2 Q_M} \right]^2 . \quad (49)$$

Figure 14 depicts the harvested power considering constant monochromatic displacement magnitude, also normalized along the x-axis with respect to the optimal load in the standard case and along the y-axis according to the maximal harvested power in the standard case, so that the chart only depends on the energy transfer efficiency γ_C and energy injection coefficient γ (respectively set to 0.9 and 0.8).

This figure clearly demonstrates the performance of the bidirectional pulsed energy extraction and injection in terms of energy harvesting, allowing a gain in terms of power output of 20 using typical components (40 using low-losses devices). Such energy scavenging abilities can be explained by a particular "energy resonance" effect, which comes from the fact that if more power is harvested, this leads to a greater injected energy, which also leads to a higher harvested power according to Eq. (41) and so on, leading to outstanding power output. It can also be noted that for low values of the load, the technique performs as the SECE technique, as almost no energy is injected to the system (the rectified voltage being low), while the power tends to zero for high load values, as higher voltages lead to higher losses.

Another remarkable property of the this technique is the fact that, when considering the damping effect introduced by the scavenging process (Figure 15), the energy extraction/injection concept allows bypassing the output power limit that is common to all the previously exposed energy harvesting approach.

Because of the voltage cancellation process, the performance of the energy extraction/injection injection technique is not significantly compromised in the case of random excitation. However, the load-dependency of the harvested power may alter the output power if the structure features several modes.

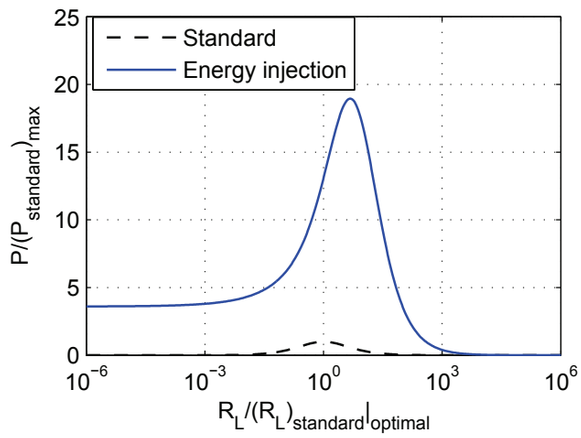

Fig. 14. Normalized harvested power of energy injection technique under constant displacement magnitude and comparison with standard interface ($\gamma = 0.8$, $\gamma_C = 0.9$)

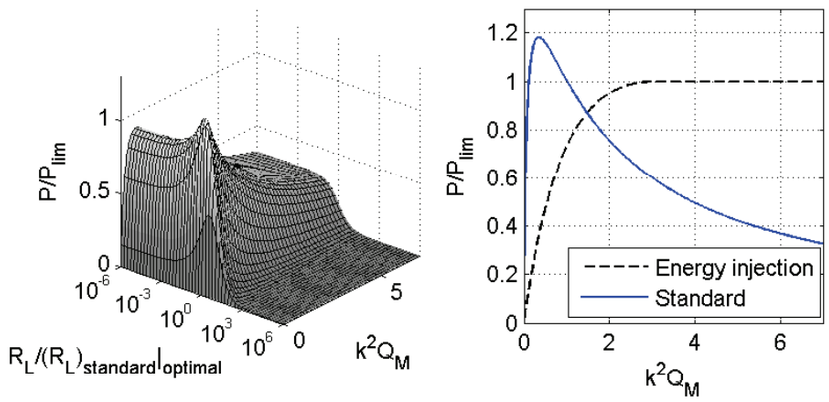

Fig. 15. Normalized harvested power and maximal normalized harvested power of energy injection technique under constant force magnitude and comparison with standard interface ($\gamma = 0.8$, $\gamma_C = 0.9$)

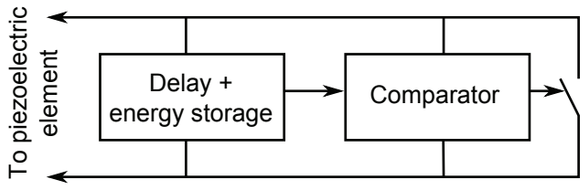

Fig. 16. Principles of the self-powered switch

6. Implementation issues

Through this chapter, it has been demonstrated that using nonlinear treatments for energy harvesting purposes allows a significant increase of the performance of vibration-based microgenerators. However, the nonlinear process may seem to be delicate to implement for realistic applications. Nevertheless, the implementation of the SSHI may be done in an easy and energy-efficient way, based on the detection of maximum values using the delayed version of the voltage (the maximum value is reached when the delayed signal becomes greater then the original piezovoltage) as depicted in Figure 16, generating a pulsed voltage that drives a transistor acting as the digital switching (Richard, Guyomar and Lefeuvre, 2007; Lallart *et al.*, 2008b). Hence, such a process can be made truly self-powered using widely available components and may be easily integrated. It besides consumes very little energy, typically 3% of the electrostatic energy available on the piezoelectric element, hence not compromising the energy harvesting enhancement offered by these techniques. The implementation of the other techniques may also be derived from this concept (Badel, 2005b; Lallart, 2008d; 2010d).

Another concerns about the implementation of piezo-based vibration harvesters is the challenge concerning low-voltage transducers, as piezoelectric elements present their most promising application field in small-scale size. However when dealing with such systems (such as MEMS[9]), the output voltage of the active material is usually very low and cannot bypass the discrete component voltage gap, leading to poor performance in terms of energy generation.

[9] *Micro Electro-Mechanical Systems*

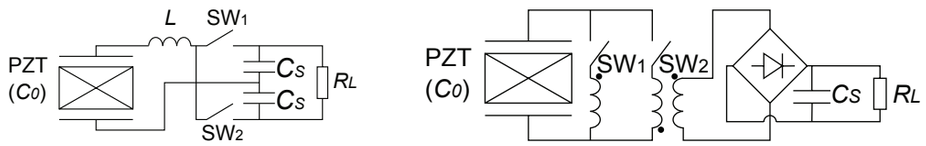

(a) Diodeless series SSHI (b) SSHI-MR

Fig. 17. Interfaces for low voltage harvesting

In order to counteract this problem, it is possible to take benefit of the nonlinear energy harvesting interfaces (Makihara, Onoda and Miyakawa, 2006; Lallart and Guyomar, 2008e). In particular, the series SSHI approach is the most flexible to be adapted to low-voltage systems. For example, the rectifier bridge may be replaced by the switching elements (Figure 17(a)), allowing the removal of the diodes. Another approach consists of replacing the switching inductance by a transformer (Figure 17(b)), leading to the concept of SSHI-MR[10] (Garbuio *et al.*, 2009), which also presents the advantage of having a higher optimal load and therefore delivers voltage levels that are compatible with electronic systems when the electromechanical structure delivers low voltage levels. Because of the load decoupling offered by the use of the transformer, the SSHI-MR technique may be combined with the parallel energy harvesting system, leading to the concept of hybrid energy harvesting (Lallart, 2008d; 2010d), which allows a decreased sensitivity to load shifts.

7. Application to thermal energy harvesting through pyroelectric effect

While the previous development have been done considering vibration energy harvesting through piezoelectric coupling, it is also possible to apply the exposed approaches to other conversion effects, as the principles of the nonlinear treatment is independent from the energy conversion mechanisms (*e.g.*, electromagnetism[11] - Lallart *et al.* (2008f)). In this section, a particular attention is placed on pyroelectric devices that are able to convert temperature variation into electricity, as these materials behave in a similar fashion than piezoelectric elements. Hence, it is possible to apply the proposed concepts to energy harvesting from temperature time-domain variations using pyroelectric inserts.

Although pyroelectric materials feature low coupling coefficients, the source presents much higher energy than mechanical vibrations. Hence, in terms of energy density, pyroelectric elements present similar energy densities than piezoelectric materials (Table 1), as the low coupling coefficient is compensated by the high input energy levels.

However, contrary to mechanical energy harvesting, thermal devices do no present any resonance effect. Combined with the low coupling coefficient of pyroelectric materials, this leads to the observation that the harvesting process does not induce a significant cooling, and hence does not significantly modify the input energy source.

From the constitutive pyroelectric equations:

$$\begin{cases} \Delta D = \epsilon_{33}^{\theta} \Delta E + p \Delta \theta \\ \Delta \sigma = p \Delta E + c \frac{\Delta \theta}{\theta_0} \end{cases}, \tag{50}$$

where θ, θ_0 and σ respectively refer to the absolute and mean temperatures in Kelvin and entropy of the system, ϵ_{33}^{θ}, p and c represent the permittivity under constant temperature,

[10] *Synchronized Switch Harvesting on Inductor with Magnetic Rectifier*

[11] In this case, the working electrical quantity is the current rather than the voltage.

	Piezoelectricity	Pyroelectricity
Material	Hard ceramic NAVY-III type ($Q\&S\ P1-89$)	PVDF films
Multiphysic coupling coefficient	$e_{33} = -12.79\ C.m^{-1}$	$p = -24.10^{-6}\ C.m^{-2}.K^{-1}$
Permittivity	$\epsilon^S{}_{33}/\epsilon_0 = 668$	$\epsilon^\theta/\epsilon_0 = 12$
Typical variation of the associated physical quantity	$S_M = 10\ \mu m.m^{-1}$	$\theta_M = 1\ K$
Associated electrostatic energy	$(W_{el})_{\text{piezo}} = 1.4\ \mu J.cm^{-3}$	$(W_{el})_{\text{pyro}} = 2.7\ \mu J.cm^{-3}$

Table 1. Electrostatic energy comparison using piezoelectric or pyroelectric coupling

pyroelectric coefficient and heat capacity, and with Δ the difference operator, it is possible to get the macroscopic model of the pyroelectric coupling (only the equation of the current is given as no significant feedback occurs):

$$I = \alpha\dot{\theta} - C_0\dot{V} \text{ with } \begin{cases} C_0 = \frac{\epsilon^\theta_{33} S_0}{l} \\ \alpha = -pS_0 \end{cases}, \tag{51}$$

with S_0 and l the surface and thickness of the material, respectively.
Hence, the output power of each technique would be the same than the previously exposed ones[12], except that the displacement magnitude u_M would be replaced by the temperature variation magnitude θ_M.
Another specificity of thermal energy harvesting from temperature time-domain variations is the low frequency of the system (less than 1 Hz typically), which leads to a decreased value of the inversion coefficient, decreasing the gain of the nonlinear techniques by a typical factor 2 approximately (Guyomar *et al.*, 2009).
This observation, combined with the fact that the system does not feature any resonance effect, shows the advantage of the SECE and DSSH techniques that offers an output power independent from the load, as low frequency variations lead to high optimal load values which can besides change easily due to the non-resonant nature of the device.

8. Conclusion

This chapter exposed the use of nonlinear treatments for energy harvesting enhancement. Thanks to the conversion magnification offered by the switching approach (allowing both a voltage increase and a reduction of the time shift between voltage and velocity), it has been demonstrated that the application of this concept to energy harvesting (SSHI) allows a

[12]Eq. (6) for the standard interface, Eqs. (16) and (24) for the parallel and series SSHI, Eqs. (33) and (37) for the SECE and DSSH approaches, and Eq. (47) for the pulsed energy injection/extraction technique.

significant gain in terms of harvested power (7-8 times greater than the standard interface) or significantly reduce the amount of piezoelectric material required to harvest a given amount of energy.
Then, the principles of a nonlinear pulsed energy extraction have been exposed, showing that such techniques not only still permits an enhancement of the output power (although they may not be as effective as SSHI approaches), but also the harvested energy is independent from the load. In particular, the use of an intermediate energy tank (DSSH) allows controlling the trade-off between energy conversion and damping effect, allowing a great reduction (typically by a factor of 10) of the required amount of piezoelement for the same amount of scavenged energy.
In a third step, the addition of a pulsed energy injection mechanism has been exposed. Thanks to the dependence of the available electrostatic energy with the squared voltage, it has been shown that providing initial energy to a piezoelectric material allows improving its conversion abilities. Applied to energy harvesting, such a process therefore allows an outstanding gain in terms of harvested power, particularly thanks to an "energy resonance" effect created by the feedback loop.
The realistic application of the switching process in a self-powered fashion has also been demonstrated, and it has been shown that such a process can simply be done by comparing the piezoelectric voltage with its delayed version, which can be implemented using widely available and embeddable components, leading to a low-consumption circuit that does not compromise the performance of the nonlinear techniques. The issue of low-voltage energy harvesting has also been discussed, as piezoelectric materials are promising for micro and nano-systems.
Finally, it has been shown that the nonlinear process may be applied to other conversion effects, as the concept is independent from the physical quantities. A particular emphasis has been placed on thermal harvesting from temperature time-domain variations using pyroelectric elements, as, although such elements feature low coupling coefficients, the source presents high energy levels. In this case, it has also been observed that the low-frequency, non-resonant nature of these systems makes the use of load-independent harvesting techniques (*e.g.*, SECE) a premium choice.
As a conclusion, Table 2 proposes a ranking of the techniques exposed in this chapter according to several criteria. Hence, it can be seen that when the system features monochromatic excitation, the use of the energy injection technique is of particular interest

Technique	Harvested energy					
	Constant displacement magnitude	Constant force magnitude	Random Excitation	Low-voltage harvesting	Load Independency	Implementation easiness
Standard	☹	☹	☹	☹	☹	☺
Parallel SSHI	☺	😐	☹	☹	☹	😐
Series SSHI (diodeless)	☺	😐	☹	😐	☹	😐
SSHI-MR	☺	😐	☹	☺	☹	😐
Hybrid SSHI	☺	😐	😐	☺	😐	😐
SECE	😐	😐	☺	😐	☺	☹
DSSH	☺	☺	😐	😐	☺	☹
Energy injection	☺☺	☺	😐	😐	😐	☹

Table 2. Comparaison of exposed energy harvesting techniques

if no vibration damping effect appears, although its self-powered implementation is not as simple as the SSHI techniques and not as efficient than the DSSH approach when damping effect appears and if the electromechanical structure features a low value of the figure of merit $k^2 Q_M$. Finally, if the system features random excitations however, the use of load-independent techniques seems more adapted.

9. References

Anton, S. R. & Sodano H. A. (2007). A review of power harvesting using piezoelectric materials (2003-2006). *Smart Mater. Struct.*, Vol. 16(3), R1-R21.

Badel, A.; Guyomar, D.; Lefeuvre, E. & Richard, C. (2005a). Efficiency Enhancement of a Piezoelectric Energy Harvesting Device in Pulsed Operation by Synchronous Charge Inversion. *J. Intell. Mater. Syst. Struct.*, Vol. 16, 889-901.

Badel, A. (2005b). Récupération dénergie et contrôle vibratoire par éléments piézoélectriques suivant une approche non linéaire[13]. Ph.D. Thesis, *in french*.

Badel, A.; Benayad, A.; Lefeuvre, E.; Lebrun, L.; Richard, C. & Guyomar, D. (2006a). Single Crystals and Nonlinear Process for Outstanding Vibration Powered Electrical Generators. *IEEE Trans. on Ultrason., Ferroelect., Freq. Contr.*, Vol. 53, 673-684.

Badel, A.; Sébald, G.; Guyomar, D.; Lallart, M.; Lefeuvre, E.; Richard, C. & Qiu, J. (2006b). Piezoelectric vibration control by synchronized switching on adaptive voltage sources: Towards wideband semi-active damping. *J. Acoust. Soc. Am.*, Vol. 119, No. 5, 2815-2825.

Badel, A.; Lagache, M.; Guyomar, D.; Lefeuvre, E. & Richard, C. (2007). Finite Element and Simple Lumped Modeling for Flexural Nonlinear Semi-passive Damping. *J. Intell. Mater. Syst. Struct.*, Vol. 18, 727-742.

Beeby, S. P.; Torah, R. N.; Tudor, M. J.; Glynne-Jones, P.; ODonnell, T.; Saha, C. R. & Roy, S. (2007). A micro electromagnetic generator for vibration energy harvesting, *J. Micromech. Microeng.*, Vol. 17, 12571265.

Blystad, L.-C. J.; Halvorsen, E. & Husa, S. (2008). Simulation of a MEMS Piezoelectric Energy Harvester Including Power Conditioning and Mechanical Stoppers. *Technical Digest, PowerMEMS 2008*, Sendai, Japan, November 2008, 237-240.

Blystad, L.-C. J.; Halvorsen, E. & Husa, S. (2010). Piezoelectric MEMS energy harvesting systems driven by harmonic and random vibrations. *IEEE Trans. Ultrason., Ferroelect., Freq. Contr.*, Vol. 57(4), 908-919.

Erturk A. & D. J. Inman (2008). Issues in mathematical modeling of piezoelectric energy harvesters. *Smart Mater. Struct. 17*, paper # 065016.

Garbuio, L.; Lallart, M.; Guyomar, D. & Richard, C. (2009). Mechanical Energy Harvester with Ultra-Low Threshold Rectification Based on SSHI Non-Linear Technique, *IEEE Trans. Indus. Elec.*, Vol. 56(4), 048-1056.

Guyomar, D.; Badel, A.; Lefeuvre, E. & Richard, C. (2005). Towards energy harvesting using active materials and conversion improvement by nonlinear processing, *IEEE Trans. Ultrason., Ferroelect., Freq. Contr.*, Vol. 52, 584-595.

Guyomar, D. & Badel, A. (2006). Nonlinear semi-passive multimodal vibration damping: An efficient probabilistic approach. *J. Sound Vib.*, Vol. 294, 249-268.

Guyomar, D.; Jayet, Y.; Petit, L.; Lefeuvre, E.; Monnier, T.; Richard, C. & Lallart, M. (2007a) Synchronized Switch Harvesting applied to Self-Powered Smart Systems :

[13] *Energy harvesting and vibration control using piezoelectric elements and a nonlinear approach*

Piezoactive Microgenerators for Autonomous Wireless Transmitters, *Sens. Act. A: Phys.*, Vol. 138, No. 1, 151-160. doi : 10.1016/j.sna.2007.04.009

Guyomar, D.; Richard, C. & Mohammadi, S. (2007b). Semi-passive random vibration control based on statistics. *J. Sound Vib.*, Vol. 307, 818-833.

Guyomar, D.; Sébald, G.; Pruvost, S.; Lallart, M.; Khodayari, A. & Richard, C. (2009). Energy Harvesting From Ambient Vibrations and Heat, *J. Intell. Mater. Syst. Struct.*, Vol. 20(5), 609-624.

Halvorsen, E. (2008). Energy Harvesters Driven by Broadband Random Vibrations. *J. Microelectromech. Syst.*, Vol. 17(5), 1061-1071.

Hamakawa, Y. (2003). 30 years trajectory of a solar photovoltaic research. In *3rd World Conference on Photovoltaic Energy Conversion*.

Han, J.; Von-Jouanne,A.; Le, T.; Mayaram, K. & Fiez, T. S. (2004). Novel power conditioning circuits for piezoelectric micro power generators. In *Proc. IEEE Appl. Power Electron. Conf. Expo. (APEC)*, vol. 3, 1541-1546.

Keawboonchuay , C. & Engel, T. G. (2003). Electrical power generation characteristics of piezoelectric generator under quasi-static and dynamic stress conditions. *IEEE Trans. Ultrason., Ferroelect., Freq. Contr.*, Vol. 50, 1377-1382.

Krikke, J. (2005). Sunrise for energy harvesting products. *IEEE Pervasive Comput.*, Vol. 4, 4-35.

Lallart, M.; Guyomar, D.; Jayet, Y.; Petit, L.; Lefeuvre, E.; Monnier, T.; Guy, P. & Richard, C. (2008a). Synchronized Switch Harvesting applied to Selfpowered Smart Systems: Piezoactive Microgenerators for Autonomous Wireless Receiver, *Sens. Act. A: Phys.*, Vol. 147, No. 1, 263-272. doi: 10.1016/j.sna.2008. 04.006.

Lallart, M.; Lefeuvre, E.; Richard, C. & Guyomar, D. (2008b). Self-Powered Circuit for Broadband, Multimodal Piezoelectric Vibration Control. *Sens. Act. A: Phys.*, Vol. 143, No. 2, 277-382, 2008. doi : 10.1016/j.sna.2007.11.017

Lallart, M.; Garbuio, L.; Petit, L.; Richard, C. & Guyomar, D. (2008c) Double Synchronized Switch Harvesting (DSSH) : A New Energy Harvesting Scheme for Efficient Energy Extraction, *IEEE Trans. Ultrason., Ferroelect., Freq. Contr.*, Vol. 55, No. 10, 2119-2130.

Lallart, M. (2008d). Amélioration de la conversion électroactive de matériaux piézoélectriques et pyroélectriques pour le contrôle vibratoire et la récupération d'énergie - Application au contrôle de santé structurale auto-alimenté[14]. Ph.D. Thesis, *in french*.

Lallart, M. & Guyomar, D. (2008e). Optimized Self-Powered Switching Circuit for Non-Linear Energy Harvesting with Low Voltage Output, *Smart Mater. Struct.*, Vol. 17, 035030. doi: 10.1088/0964-1726/17/3/035030

Lallart, M.; Magnet, C.; Richard, C.; Lefeuvre, E.; Petit, L.; Guyomar, D. & Bouillault, F. (2008f). New Synchronized Switch Damping Methods Using Dual Transformations. *Sens. Act. A: Phys.*, Vol. 143, No. 2, 302-314. doi : 10.1016/j.sna.2007.12.001

Lallart, M.; Inman, D. J. & Guyomar, D. (2010a - *in press - available online*). Transient Performance of Energy Harvesting Strategies under Constant Force Magnitude Excitation. *J. Intell. Mater. Syst. Struct.*. DOI: 10.1177/1045389X09358334.

Lallart, M. & Inman, D. J. (2010b). Low-Cost Integrable Tuning-Free Converter for Piezoelectric Energy Harvesting Optimization. *IEEE Trans. Power Electron.*, Vol. 25(7), 1811 - 1819.

Lallart, M. & Guyomar, D. (2010c). Piezoelectric conversion and energy harvesting enhancement by initial energy injection. Appl. Phys. Lett., Vol. 97, # 014104.

[14] *Electroactive conversion enhancement of piezoelectric and pyroelectric materials for vibration control and energy harvesting - Application to self-powered Structural Health Monitoring*

Lallart, M. (2010d). Conversion électroactive et application aux systèmes auto-alimentés[15]. Editions Universitaires Européennes, *in french*. ISBN: 978-613-1-50507-2

Lefeuvre, E.; Badel, A.; Richard, C. & Guyomar, D. (2005). Piezoelectric energy harvesting device optimization by synchronous electric charge extraction. *J. Intell. Mat. Syst. Struct.*, Vol. 16, No. 10, 865-876.

Lefeuvre, E.; Badel, A.; Richard, C.; Petit, L. & Guyomar, D. (2006a). A comparison between several vibration-powered piezoelectric generators for standalone systems, *Sens. Act. A: Phys*, Vol. 126, 405-416.

Lefeuvre, E.; Badel, A.; Petit, L.; Richard, C. & Guyomar D. (2006b). Semi-passive Piezoelectric Structural Damping by Synchronized Switching on Voltage Sources. *J. Intell. Mater. Syst. Struct.*, Vol. 17, Nos. 8-9, 653-660.

Lefeuvre, E.; Audigier, D.; Richard, C. & Guyomar, D. (2007a). Buck-boost converter for sensorless power optimization of piezoelectric energy harvester. *IEEE Trans. Power Electron.*, Vol. 22(5), 2018-2025.

Lefeuvre, E.; Badel, A.; Richard, C. & Guyomar, D. (2007b). Energy harvesting using piezoelectric materials: Case of random vibrations. *J. Electrocem.*, Vol. 19(4), 349-355.

Liang, J. R. & Liao, W. H. (2009). An Improved Self-Powered Switching Interface for Piezoelectric Energy Harvesting. In *Proc. of 2009 IEEE International Conference on Information and Automation*, 945-950.

Makihara, K.; Onoda, J. & Miyakawa, T. (2006). Low energy dissipation electric circuit for energy harvesting. *Smart Mater. Struct.*, Vol. 15, 1493-1498.

T. H. Ng, T. H.& Liao, W. H. (2005). Sensitivity Analysis and Energy Harvesting for a Self-Powered Piezoelectric Sensor. *J. Intell. Mat. Syst. Struct.*, Vol. 16(10), 785-797.

Ottman, G. K.; Hofmann, H. F.; Bhatt, A. C. & Lesieutre, G. A. (2002). Adaptive Piezoelectric Energy Harvesting Circuit for Wireless Remote Power Supply. *IEEE Trans. Power Electron.*, vol. 17(5), 669-676.

Ottman, T. S.; Hofmann, H. F. & Lesieutre, G. A. (2003). Optimized piezoelectric energy harvesting circuit using step-down converter in discontinuous conduction mode. *IEEE Trans. Power Electron.*, Vol. 18(2), 696-703.

Paradiso, J. A. & Starner, T. (2005). Energy scavenging for mobile and wireless electronics. *IEEE Pervasive Computing*, Vol. 4, 18-27.

Park, S.-E. & Hackenberger, W. (2002). High performance single crystals, applications and issues. *Current Opinion in Solid State and Material Science*, Vol. 6, 11-18.

Petit, L.; Lefeuvre, E.; Richard, C. & Guyomar, D. (2004). A broadband semi passive piezoelectric technique for structural damping, *Proceedings of SPIE conference on Smart Struct. Mater. 1999: Passive Damping and Isolation*, San Diego, CA, USA, March 2004, Vol. 5386, 414-425. ISBN : 0-8194-5303-X

Qiu, J.; Ji, H. & Zhu, K. (2009a). Semi-active vibration control using piezoelectric actuators in smart structures. *Front. Mech. Eng. China*, Vol. 4(3), 242-251.

Qiu, J.; Jiang, H.; Ji, H. & Zhu, K. (2009b). Comparison between four piezoelectric energy harvesting circuits. *Front. Mech. Eng. China*, Vol. 4(2), 153-159.

Richard, C.; Guyomar, D.; Audigier, D. & Ching, G. (1999). Semi passive damping using continuous switching of a piezoelectric device, *Proceedings of SPIE conference on Smart Struct. Mater. 1999: Passive Damping and Isolation*, Newport Beach, CA, USA, March 1999, Vol. 3672, 104-111. ISBN : 0-8194-3146-X

Richard C.; Guyomar, D. & Lefeuvre, E. (2007). Self-Powered Electronic Breaker With

[15] *Electroactive conversion and application to self-powered systems*

Automatic Switching By Detecting Maxima Or Minima Of Potential Difference Between Its Power Electrodes, *patent # PCT/FR2005/003000*, publication number: WO/2007/063194, 2007.

Richards, C. D.; Anderson, M. J.; Bahr, D. F. & Richards, R. F. (2004). Efficiency of energy conversion for devices containing a piezoelectric component. *J. Micromech. Microeng.*, Vol. 14, 717-721.

Roundy, S. & Wright, P. K. (2004). A piezoelectric vibration based generator for wireless electronics. *Smart Mater. Struct.*, Vol. 13, 1131-1142.

Shearwood C. & Yates, R. B. (1997). Development of an electromagnetic microgenerator. *Electronics Letters*, Vol. 33, 1883-1884.

Shu, Y. C.; Lien, I. C. & Wu, W. J. (2007). An improved analysis of the SSHI interface in piezoelectric energy harvesting. *Smart Mater. Struct.*, Vol. 16, 2253-2264.

Sodano, H. A.; Simmers, G. E.; Dereux, R. & Inman, D. J. (2006). Recharging batteries using energy harvested from thermal gradients. *J. Intell. Mater. Syst. Struct.*, Vol. 18, 4-10.

Taylor, G. W.; Burns, J. R.; Kammann, S. M.; Powers, W. B. & Welsh, T. R. (2001). The Energy Harvesting Eel: A Small Subsurface Ocean/River Power Generator. *IEEE J. Oceanic Eng.*, Vol. 26, 539-547.

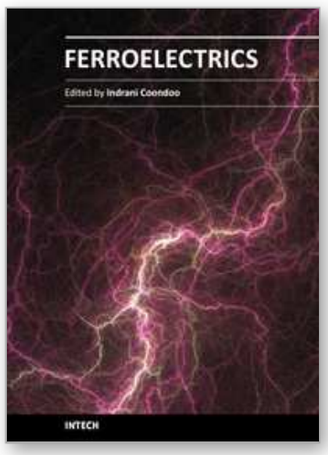

Ferroelectrics

Edited by Dr Indrani Coondoo

ISBN 978-953-307-439-9
Hard cover, 450 pages
Publisher InTech
Published online 14, December, 2010
Published in print edition December, 2010

Ferroelectric materials exhibit a wide spectrum of functional properties, including switchable polarization, piezoelectricity, high non-linear optical activity, pyroelectricity, and non-linear dielectric behaviour. These properties are crucial for application in electronic devices such as sensors, microactuators, infrared detectors, microwave phase filters and, non-volatile memories. This unique combination of properties of ferroelectric materials has attracted researchers and engineers for a long time. This book reviews a wide range of diverse topics related to the phenomenon of ferroelectricity (in the bulk as well as thin film form) and provides a forum for scientists, engineers, and students working in this field. The present book containing 24 chapters is a result of contributions of experts from international scientific community working in different aspects of ferroelectricity related to experimental and theoretical work aimed at the understanding of ferroelectricity and their utilization in devices. It provides an up-to-date insightful coverage to the recent advances in the synthesis, characterization, functional properties and potential device applications in specialized areas.

InTech Europe
University Campus STeP Ri
Slavka Krautzeka 83/A
51000 Rijeka, Croatia
Phone: +385 (51) 770 447
Fax: +385 (51) 686 166
www.intechopen.com

InTech China
Unit 405, Office Block, Hotel Equatorial Shanghai
No.65, Yan An Road (West), Shanghai, 200040, China
中国上海市延安西路65号上海国际贵都大饭店办公楼405单元
Phone: +86-21-62489820
Fax: +86-21-62489821

IntechOpen